The EMBO Journal vol.14 no.11 pp.2447–2460, 1995

# Epitope mapping and direct visualization of the parallel, in-register arrangement of the double-stranded coiled-coil in the NuMA protein

**Jens Harborth, Klaus Weber and Mary Osborn[1]**

Max Planck Institute for Biophysical Chemistry, Department of Biochemistry, PO Box 2841, D-37018 Goettingen, Germany

[1]Corresponding author

**NuMA, a 238 kDa protein present in the nucleus during interphase, translocates to the spindle poles in mitosis. NuMA plays an essential role in mitosis, since microinjection of the NuMA SPN-3 monoclonal antibody causes mitotic arrest and micronuclei formation. We have mapped the approximate position of the epitopes of six monoclonal NuMA antibodies using recombinant NuMA fragments. The SPN-3 epitope has been located to residues 255–267 at the C-terminus of the first helical subdomain of the central rod domain and several residues crucial for antibody binding have been identified. To gain insight into the ultrastructure of NuMA, several defined fragments, as well as the full-length recombinant protein, were expressed in *Escherichia coli* and purified to homogeneity. They were then characterized by chemical cross-linking, circular dichroism spectra and electron microscopy. The results directly reveal the tripartate structure of NuMA. A long central rod domain is flanked by globular end domains. The rod is 207 nm long and is at least 90% α-helical. It reflects a double-stranded coiled-coil with the α-helices arranged parallel and in register. The NuMA protein thus forms the longest coiled-coil currently known. Our analyses reveal no indication that recombinant NuMA assembles into filaments or other higher order structures.**

*Key words*: coiled-coil/cross-linking/electron microscopy/epitope location/NuMA

## Introduction

The nuclear mitotic apparatus protein (NuMA) changes its cellular location in a cell cycle-specific manner. In interphase NuMA is associated with the nuclear matrix (Lydersen and Pettijohn, 1980; Price and Pettijohn, 1986; Kallajoki *et al.*, 1991). In mitosis it relocates to the spindle poles. NuMA has been cloned and fully sequenced (Compton *et al.*, 1992; Yang *et al.*, 1992; Maekawa and Kuriyama, 1993; Tang *et al.*, 1993). These sequences, as well as partial nucleotide or amino acid sequences from other laboratories, show that a variety of other antigens originally given different names are in fact the NuMA molecule. These include SPN (Kallajoki *et al.*, 1991, 1993), SP-H (Maekawa *et al.*, 1991), centrophilin (Tousson *et al.*, 1991), W1 (Tang *et al.*, 1993) and 1H1/1F1 (Compton *et al.*, 1991).

Micronucleation and mitotic arrest as consequences of injection of a NuMA antibody were first described for the SPN-3 antibody. Approximately 50% of HeLa cells became micronucleated after injection of SPN-3 antibodies and this effect was seen at antibody concentrations as low as 300 μg/ml. The other 50% became blocked in mitosis and displayed aberrant spindles, as judged by staining with tubulin antibodies. These results allowed us to conclude that the NuMA/SPN antigen plays a functional role in mitosis (Kallajoki *et al.*, 1991, 1993). Other evidence arguing that this is the case includes the demonstration by Yang and Snyder (1992) that injection of a rabbit NuMA antibody into cells in early mitotic stages prevented spindle formation, while injection into metaphase cells caused the collapse of the mitotic spindle. Compton and Cleveland (1993) have shown that the defect in the hamster cell line tsBN2, which forms micronuclei at the restrictive temperature, can be rescued by expression of human NuMA. These authors have also shown that transfection of hamster BHK-21 cells with cDNA constructs encoding truncated forms of the human NuMA protein can lead to micronucleation. Thus there is substantial evidence from several laboratories that a correctly functioning NuMA protein is essential for mitosis and nuclear reformation.

Secondary structure prediction rules indicate that the NuMA polypeptide should have a very long α-helical domain flanked by non-helical terminal domains (Compton *et al.*, 1992; Yang *et al.*, 1992). In this respect NuMA is similar to the molecules that constitute the building blocks of the cytoplasmic intermediate filaments and of the nuclear lamins (Fuchs and Weber, 1994).

Our objectives in the work described here were threefold. First, to identify the exact position of the epitope of the SPN-3 monoclonal antibody along the NuMA polypeptide chain and compare it with that of other NuMA antibodies which do not result in aberrant spindle formation or in micronuclei formation when injected into cells. Second, to decide whether NuMA indeed belongs to the coiled-coil proteins and the number and arrangements of the helices used to build the putative coiled-coil. Third, to describe the ultrastructure of purified NuMA by electron microscopy and to explore whether NuMA can, by analogy with intermediate filament proteins, also form filaments *in vitro*. For this purpose several defined NuMA fragments, as well as full-length NuMA, have been expressed as recombinant proteins in *Escherichia coli*. The purified NuMA derivatives have been characterized by chemical cross-linking experiments, circular dichroism (CD) spectra and electron microscopy. The combined results document the NuMA molecule as a long thin rod with a coiled-coil length of ~210 nm in which two α-helices are arranged in parallel and in register. The SPN-3 epitope locates to the C-terminus of the first helical subdomain of the central rod domain.

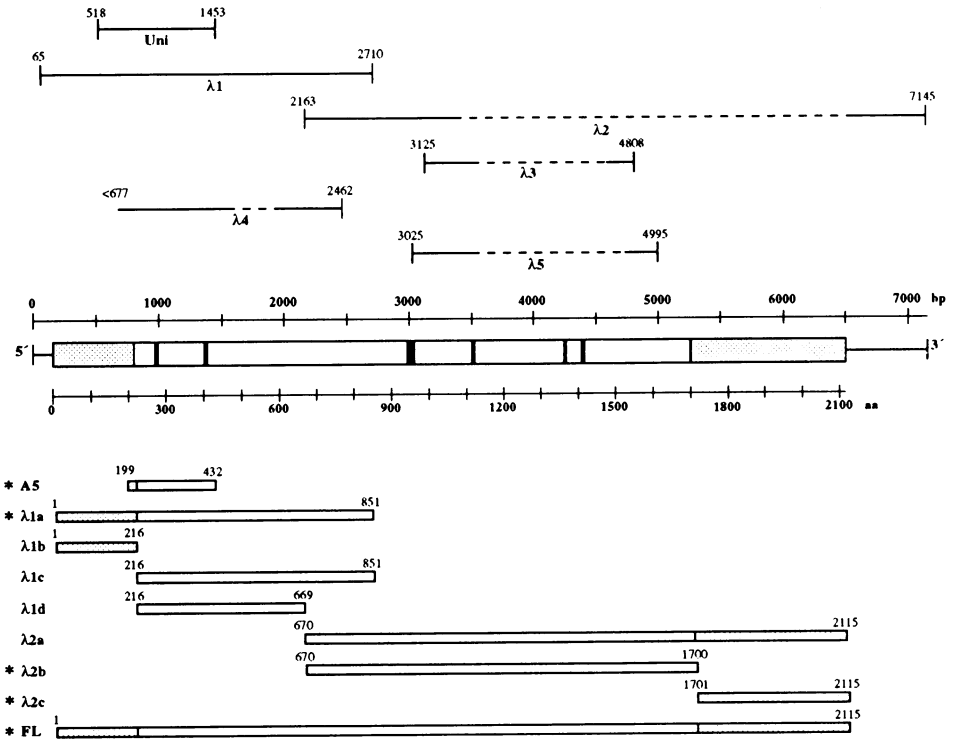


**Fig. 1.** (Centre) The base pair positions, amino acid positions and secondary structure of the NuMA protein proposed from the cDNA sequence (Compton *et al.*, 1992; Yang *et al.*, 1992). Precise positions are taken from Yang *et al.* (1992). Note the long central α-helical region (rod) consisting of several helical subdomains. Interruptions by one or more proline residues are indicated by solid vertical bars. Note the globular head and tail domains at the N- and C-terminal ends (shaded). (Top) Positions of the overlapping NuMA cDNA clones isolated in this study from HeLa cDNA libraries in Uni-Zap XR or λ ZAP II vectors. Solid lines represent those regions that have been completely sequenced in this study. The boundaries of the clones are indicated by vertical bars. (Bottom) Relative positions of the recombinant clones, which were ligated in the pRSET vector and expressed as fusion proteins in *E.coli*. The corresponding amino acid positions are indicated above each fragment. The full-length expression clone (FL) was derived from the overlapping λ1a and λ2a fragments. *, fragments examined in the electron microscope.

## Results

### *Isolation of cDNA clones covering the entire human NuMA protein*

The central part of Figure 1 indicates the organization of the NuMA molecule inferred from its sequence and from the use of secondary structure prediction rules (Compton *et al.*, 1992; Yang *et al.*, 1992). Numbering is according to Yang *et al.* (1992). The predicted structure of the NuMA molecule includes a long central α-helical region interrupted at six different points by one or more proline residues. This region is flanked by putative globular head and tail domains. Figure 1 also shows the relative positions of the cDNA constructs and the recombinant protein fragments used in this study.

The cDNA clones Uni and λ1–5 were isolated by screening plaques from two commercially available HeLa cell expression libraries with a mixture of six NuMA monoclonal antibodies (SPN-1 to -5 and SPN-7) (Kallajoki *et al.*, 1991). Two clones from the Uni-Zap XR library (out of 1 200 000 phages plated) and five clones from the λ Zap II library (out of 600 000 phages plated) which reacted positively with the antibody mixture were selected for further characterization. DNA sequencing showed that the two clones from the Uni-Zap library were identical. The Uni clone and the λ1 clone were fully sequenced, while for the other λ clones sufficient sequences were obtained to establish the clone boundaries shown in the top part of Figure 1. The regions that we sequenced (Figure 1, solid lines) were all identical with the NuMA sequence of Yang *et al.* (1992). Each cDNA clone was purified and expressed as a β-galactosidase (β-gal) fusion protein in *E.coli*.

Several mutants of the λ1 clone (λ1a–d), the λ2 clone (λ2a–c) and the Uni clone (A5) were generated using PCR and cloned into pRSET expression plasmids. This allowed bacterial expression of a set of fusion proteins corresponding to the different structural domains of the NuMA molecule. Thus the λ1b fragment covers the head domain, which is predicted to be globular, while the λ1c fragment includes only the part of λ1 thought to form an α-helix. The λ2b fragment covers the part of λ2 thought to be α-helical, while the λ2c fragment spans the tail region, which is thought to be a globular domain. These constructs are shown diagrammatically in the lower part of Figure 1. To construct the full-length NuMA cDNA we used a unique *Bst*EII site located within the overlapping region of the λ1 and λ2 clones. The appropriate fragments were generated and cloned into the pRSET expression vector, as described in Materials and methods.

### *Position of the epitopes recognized by the different SPN antibodies*

*Escherichia coli* extracts expressing NuMA derivates either as β-gal or as pRSET fusion proteins were tested in a dot blot with each of the six SPN/NuMA antibodies (Table I). For example, in the first test against the β-gal

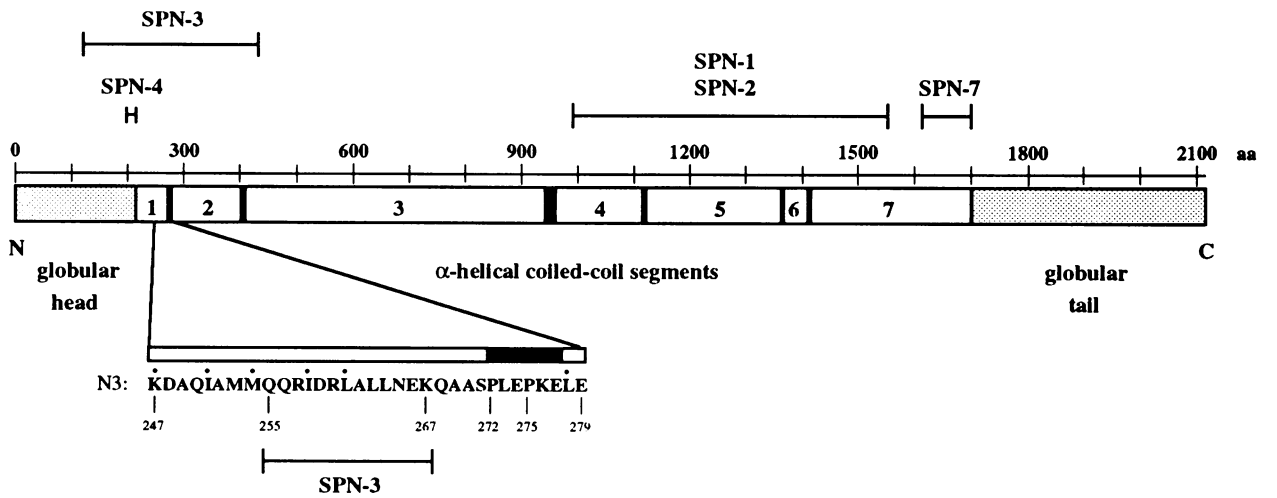


**Fig. 2.** Approximate locations of the SPN-1, -2, -3, -4 and -7 epitopes (top) and the precise position of the SPN-3 epitope (bottom) along the NuMA polypeptide. Epitopes, marked by horizontal bars, were located approximately using the results in Table I. The precise location of the SPN-3 epitope was obtained from the reactivity of the recombinant fragments in Figure 3 and of the synthetic peptides in Table II. The SPN-3 antibody reacted with the protein product of the N3 clone. Its sequence of 33 amino acids was determined and is given at the bottom of the figure. Using the series of overlapping synthetic peptides shown in Table II the SPN-3 epitope was located to the C-terminal end of the first α-helical subdomain of the central rod. The epitope corresponds to residues 255–267 of the NuMA protein (see Figure 4). The dots above the N3 sequence indicate the a and d positions of the consecutive heptads which are generally occupied by hydrophobic residues. Note the break in the helix following the SPN-3 epitope. It is marked by two proline residues at positions 272 and 275.

fusion proteins, SPN-1 and SPN-2 reacted strongly with the extracts expressing λ2, λ3 and λ5, but not with those expressing Uni, λ1 or λ4. In the second test against the pRSET fusion proteins, SPN-1 and SPN-2 reacted with the λ2a and λ2b fragments and the full-length NuMA molecule, but not with the other fragments. The SPN-1 and SPN-2 epitopes are therefore located within the C-terminal portion of the NuMA rod, i.e. between residues 991 and 1550 (Figure 2). Similarly, the results in Table I allow the SPN-4 epitope to be located to the region between amino acid residues 199 and 216 of the NuMA molecule, i.e. to the extreme C-terminus of the globular head domain. The SPN-7 epitope lies between residues 1613 and 1700 at the C-terminus of the coiled-coil region. Since SPN-5 reacted with λ1a, but not with λ1b, λ1c or λ1d, the epitope of this antibody either lies at the junction of λ1b and λ1c or, alternatively, it is a non-linear epitope. The smallest of the original NuMA clones recognized by the SPN-3 antibody is the Uni-clone (amino acids 122–432, Table I). Since SPN-3 reactivity is retained by λ1c and λ1d, which both start at residue 216, the SPN-3 epitope must lie between residues 216 and 432. Information on epitopes of the different SPN antibodies, derived from the data in Table I, is shown in the top part of Figure 2.

**Table I.** Reactivity of the recombinant proteins with the six NuMA antibodies SPN-1 to 5 and SPN-7

| | Antibodies | | | | | |
|---|---|---|---|---|---|---|
| | SPN-1 | SPN-2 | SPN-3 | SPN-4 | SPN-5 | SPN-7 |
| β-gal fusion proteins | | | | | | |
| Uni | – | – | + | + | ? | – |
| λ1 | – | – | + | + | ? | – |
| λ2 | + | + | – | – | – | + |
| λ3 | + | + | – | – | – | – |
| λ4 | – | – | + | + | ? | – |
| λ5 | + | + | – | – | – | – |
| pRSET fusion proteins | | | | | | |
| A5 | – | – | + | + | ? | – |
| λ1a | – | – | + | + | + | – |
| λ1b | – | – | – | + | – | – |
| λ1c | – | – | + | – | – | – |
| λ1d | – | – | + | – | – | – |
| λ2a | + | + | – | – | – | + |
| λ2b | + | + | – | – | – | + |
| λ2c | – | – | – | – | – | – |
| FL | + | + | + | + | + | + |

### *Determination of the epitope recognized by the SPN-3 antibody*

The SPN-3 antibody, but not the SPN-1, -2, -4 or -5 antibodies, caused aberrant spindle formation and micronuclei formation when microinjected into HeLa cells (Kallajoki *et al.*, 1991, 1992, 1993). Therefore, the exact location of the SPN-3 epitope was of particular interest. The strategy used to identify it is shown in Figure 3 and Table II and involved analysis of recombinant protein fragments and of synthetic peptides.

*Recombinant protein fragments.* The smallest of the original cDNA clones which, when expressed in *E.coli*, reacted with the SPN-3 antibody was the Uni clone (Table I). It has a size of 936 bp and encompasses residues 518–1453 in the NuMA cDNA sequence and therefore corresponds to amino acids 122–432 of the NuMA protein. The subcloning strategy used the NuMA DNA of the Uni clone to amplify overlapping fragments by PCR, which were cloned into the T7 expression vector pRSET A. In a first round of subcloning, five subfragments, A1–A5, were generated, of which A2, A4 and A5 reacted with the SPN-3 antibody (e.g. Figure 3, lanes 2 and 3). A second round of cloning used as template the smallest fragment that reacts with the SPN-3 antibody, i.e. A2 (Figure 3A). This contains bp 751–1074 of the NuMA cDNA sequence and corresponds to residues 199–306 in

the amino acid sequence. In the second round, seven overlapping constructs, N1–N7, were expressed and screened with SPN-3 antibody. Only three reacted in an immunoblot (Figure 3A). The smallest of these positive clones, N3, corresponds to bp 895–993 of the NuMA sequence and this assignment was confirmed by DNA sequencing. The N3 fragment codes for the 33 amino acid residue fragment KDAQIAMMQQRIDRLALLNEKQA-ASPLEPKELE, which spans residues 247–279 in the NuMA sequence. Thus the SPN-3 epitope locates to a region which spans the C-terminal half of the first putative coiled-coil segment and the adjacent linker sequence of the NuMA rod domain (see lower part of Figure 2). The dots in Figure 2 indicate the residues in the heptad positions a and d, which participate in the putative coiled-coil formation. To confirm this epitope location further, the N3 fragment (NuMA residues 247–279) was expressed as a fusion protein using pRSET A and isolated by nickel–nitrilotriacetate (Ni–NTA) affinity chromatography (Figure 3B, lanes 4 and 5). The purified N3 fragment reacted with the SPN-3 antibody (Figure 3B, lane 6). Amino acid sequence analysis using lysine protease-derived peptides and CNBr fragments confirmed the presence of NuMA residues 247–279 (data not shown).

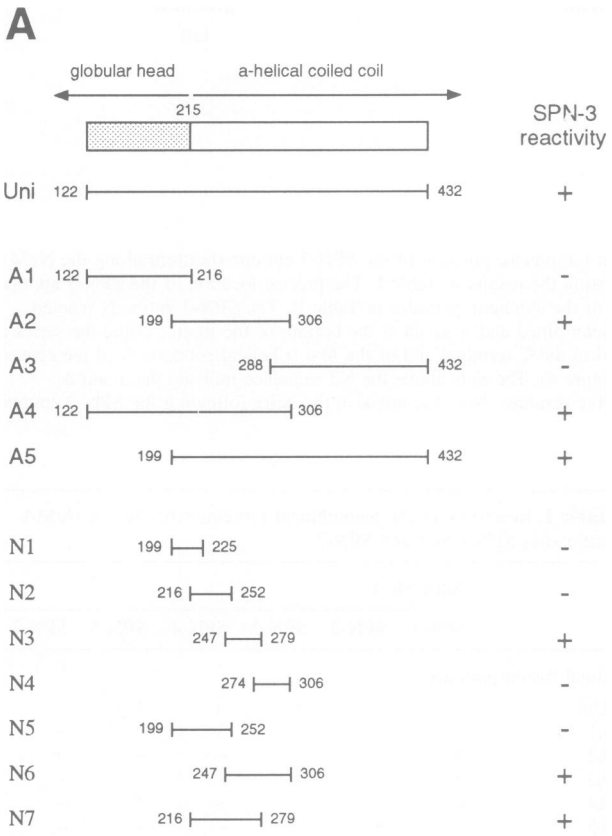


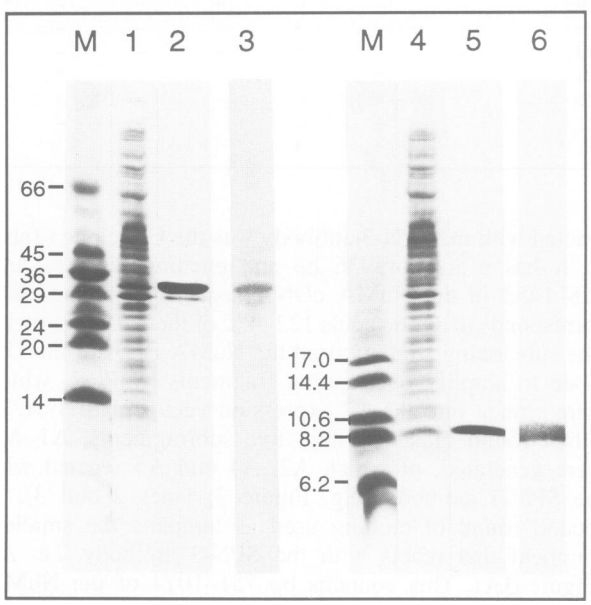


*Synthetic peptides.* The SPN-3 epitope was further delineated using a series of overlapping synthetic peptides covering the N3 fragment (residues 247–279) (Table II). In the first set of experiments three peptides were synthesized: peptide 1 (residues 247–264), peptide 2 (residues 255–271) and peptide 3 (residues 262–279). In dot blots of the peptides coupled to ovalbumin, only peptide 2 reacted with the SPN-3 antibody. In a competitive ELISA with the NuMA λ1a fragment (amino acid residues 1–851), again only peptide 2 showed a strong reaction with the SPN-3 antibody, while peptides 1 and 3 did not. Thus the SPN-3 epitope must be within residues 255–271 (Table II). In the second set of experiments synthetic peptides with deletions at either the N-terminal or the C-terminal side of peptide 2 were used. Of the three different N-terminal derivatives, only peptide 9 reacted with SPN-3 in the dot blot. This peptide also showed competitive inhibition with the λ1a fusion protein in the ELISA assay (Table II). Of the four C-terminal derivatives shown in Table II, peptides 25, 26 and 29 reacted with SPN-3 in the dot blot and showed competitive inhibition with the λ1a fusion protein in the ELISA assay. The combined results show that the tridecapeptide QQRIDRLALLNEK (residues 255–267 of NuMA) harbours the SPN-3 epitope.

To identify single amino acid residues involved in the formation of the SPN-3 epitope a third set of experiments

**Fig. 3.** SPN-3 reactivity of recombinant NuMA fragments. (**A**) The diagram at the top shows part of the globular head domain followed by the first part of the central rod domain. The Uni clone (amino acids 122–432) was the smallest clone isolated from the libraries which reacted with SPN-3 (Table I). The overlapping subclones A1–A5 were generated by PCR from the Uni clone. The A2 clone (amino acids 199–306) was the smallest derivative retaining SPN-3 reactivity. The overlapping subclones N1–N7 were generated by PCR from the A2 derivative. N3 (amino acids 247–279) was the smallest construct which when expressed reacted positively with SPN-3. Clones are indicated as horizontal bars and the corresponding terminal residues of the NuMA sequence are indicated. Reactivities of the pRSET fusion proteins (A1–A5 and N1–N7) with the SPN-3 antibody are indicated on the right. The position of the 33 residues of the N3 protein in the NuMA sequence is shown in Figure 2. All constructs shown in (A) were expressed in *E.coli* and separated on tricine–SDS–PAGE. (**B**) Expression and purification of the A5 fragment (lanes 1–3) and of the N3 fragment (lanes 4–6). Lanes 1, 2, 4 and 5 show Coomassie blue stained tricine–SDS–PAGE gels. Lanes 1 and 4, cell lysate after 4 h expression; lanes 2 and 5, purified fusion protein after Ni–NTA chromatography and HPLC; lanes 3 and 6, immunoblot of the purified A5 and N3 fragments with SPN-3 antibody. The sizes of the marker proteins are given in kDa on the left.

**Table II.** Reactivity of the synthetic peptides used to define the epitope of the SPN-3 antibody

| Pep. No. | Position in NuMA sequence | Sequence | Dot blot SPN-3 | c.E. |
|---|---|---|---|---|
| N3 | 247-279 | KDAQIAMMQQRIDRLALLNEKQAASPLEPKELE | | |
| 1 | 247-264 | CKDAQIAMMQQRIDRLALL | - | - |
| 2 | 255-271 | CQQRIDRLALLNEKQAAS | +++ | 15 |
| 3 | 262-279 | CALLNEKQAASPLEPKELE | - | - |
| **N-terminal end** | | | | |
| 9 | 255-270 | QQRIDRLALLNEKQAAC | ++ | 140 |
| 10 | 256-270 | QRIDRLALLNEKQAAC | - | 500 |
| 11 | 257-270 | RIDRLALLNEKQAAC | - | - |
| **C-terminal end** | | | | |
| 25 | 255-268 | CQQRIDRLALLNEKQ | +++ | 12 |
| 26 | 255-267 | CQQRIDRLALLNEK | +++ | 10 |
| 27 | 255-266 | CQQRIDRLALLNE | - | - |
| 29 | 255-267 | QQRIDRLALLNEKC | + | 400 |
| 2 | 255-271 | CQQRIDRLALLNEKQAAS | +++ | 15 |
| **Point mutations** | | | | |
| 19 | 255 Q→A | CA..... | +/- | 100 |
| 36 | 255 Q→N | CN..... | + | 80 |
| 20 | 256 Q→A | C.A..... | +++ | 5 |
| 4 | 257 R→A | M..A..... | | 70 |
| 34 | 257 R→A | C..A..... | + | 35 |
| 21 | 258 I→E | C...E..... | + | 120 |
| 30 | 258 I→A | C...A..... | ++ | 17 |
| 5 | 259 D→A | M....A..... | | - |
| 22 | 259 D→E | C....E..... | - | - |
| 6 | 260 R→A | M.....A..... | | - |
| 23 | 260 R→K | C.....K..... | - | - |
| 14 | 261 L→E | C......E.....G | - | 230 |
| 31 | 261 L→A | C......A..... | + | 100 |
| 15 | 262 A→E | C.....E.....G | ++ | 50 |
| 16 | 263 L→E | C.....E.....G | - | - |
| 32 | 263 L→A | C.....A..... | + | 80 |
| 17 | 264 L→E | C.....E....G | - | - |
| 33 | 264 L→A | C.....A..... | + | 110 |
| 18 | 265 N→G | C.....G...G | ++ | 30 |
| 7 | 266 E→A | M.....A..... | | 40 |
| 35 | 266 E→A | C.....A..... | +++ | 40 |
| 8 | 267 K→A | M.....A.... | | 200 |
| 28 | 267 K→A | C.....A.... | +/- | 200 |
| 24 | 267 K→R | C.....R.... | ++ | 30 |

c.E.: competitive ELISA

The top line gives the sequence of N3 (NuMA positions 247–279), which was the smallest recombinant fragment to react with the SPN-3 antibody. Of the overlapping peptides 1–3, which together cover the N3 sequence, only peptide 2 (positions 255–271) retained SPN-3 reactivity. Peptides 9–11 and peptides 25–27 and 29 were used to define the N- and C-terminal borders of the epitope. The additional cysteine present either at the N- or the C-terminal end was used to couple the peptides with Sulfo-MBS to ovalbumin. The combined results show that SPN-3 reactivity was retained in the sequence 255–267. The lower part of the table lists the synthetic peptides in which a single amino acid in the NuMA sequence between residues 255 and 267 was systematically replaced. Reactivity of the peptides coupled to ovalbumin via an additional cysteine residue was measured in a dot blot assay. +++ a strong reaction with the SPN-3 antibody; ++ a good reaction; + a weaker reaction; – no reaction. Reactivities were also tested in a competitive ELISA with the λ1a fragment and the SPN-3 antibody (for details see Materials and methods). The peptide concentration (μM) neccessary for 50% competition is shown in the last column. The symbol – means that at the highest peptide concentration tested (1 mM) 50% competition was not yet achieved. For a summary of these results see Figure 4.

used synthetic peptides with a single amino acid replacement in each of the 13 residues of the NuMA sequence covering residues 255–267. The mutant peptides were assayed with SPN-3 in the dot blot assay or in a competitive ELISA (Table II). As shown in Table II and summarized in Figure 4, various positions (Q256, R257, I258, L261, L263, L264 and E266) could be replaced by alanine without loss of antibody reactivity, which is often found in α-helices forming coiled-coils. In the case of D259 and R260, replacement by alanine abolished SPN-3 reactivity, while replacement of Q255 and K267 led to reduced reactivity. More striking were the results of the conservative replacements of D259 and R260 by glutamic acid and lysine respectively, which led to a loss of antibody reactivity (Table II, Figure 4). Other mutations which abolished antibody reactivity involved the replacement of the three leucines by glutamic acid, while I258 could be substituted by glutamic acid without loss of reactivity.

In summary, the SPN-3 epitope (residues 255–267) lies towards the N-terminal end of the large NuMA molecule (2115 residues). It is located at the C-terminal end of the predicted first helical subdomain (residues 216–271) of the central rod domain (residues 216–1700). Amino acid replacement studies of the tridecapeptide showed that D259 and R260 do not allow a conservative replacement without loss of antibody reactivity, while some other positions seemed less sensitive.

To explore whether the synthetic peptide including the SPN-3 epitope could adopt an α-helical conformation we measured the CD of peptide 2. The peptide showed no structure in phosphate-buffered saline, but the addition of 50% trifluoroethanol induced 79% α-helix (Figure 6A).

### *Purification and physical properties of the recombinant fragments and of full-length recombinant NuMA protein*

The cDNA sequence predicts that the NuMA polypeptide contains a long central coiled-coil domain which spans residues 216–1700 and has a length of ~220 nm (Parry, 1994). To see if we could provide experimental evidence in support of this structure we tried initially to measure certain physical properties of the native antigen in crude

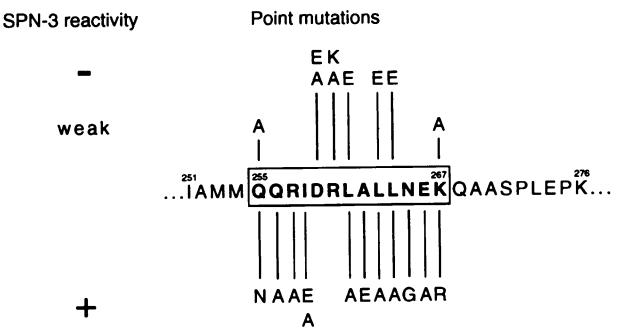


**Fig 4.** Amino acid replacements in the SPN-3 epitope. The sequence corresponding to residues 251–276 of the NuMA sequence is shown in the centre. The smallest synthetic peptide recognized by the SPN-3 antibody, the tridecapeptide spanning residues 255–267 (Table II), is boxed. The epitope was further characterized using synthetic peptides, each of which contained a single point mutation. Peptides with the single replacement given at the top of the figure showed either no or a very weak reactivity with the SPN-3 antibody. Peptides with the single replacement given at the bottom retained SPN-3 reactivity (for details see Table II).

extracts. Measurement of the sedimentation coefficient in a sucrose gradient, monitored by a dot blot assay, gave a value of 5.7 S. Gel permeation chromatography revealed a viscosity radius of 23 nm. These values suggest that NuMA is an asymmetric rod-like molecule.

Since it was difficult to obtain enough NuMA protein for physical studies from extracts of mitotic HeLa cells, we decided to purify recombinant NuMA fragments, as well as the full-length recombinant NuMA protein, from *E.coli* and to use this material to study the physical properties of NuMA. Different fragments of NuMA were expressed in the pRSET vector. The pRSET vector is a T7 RNA polymerase-driven expression system that encodes recombinant proteins as fusions with a multifunctional leader peptide containing a hexahistidyl sequence (His-tag) to allow purification on $Ni^{2+}$ affinity resins. The leader peptide also contains amino acids 1–12 of the T7 gene 10 major capsid protein, which allows the immunological detection of pRSET-expressed fusion proteins (Kroll *et al.*, 1993). Since all NuMA derivatives were cloned 5′ into the *Bam*HI site of the polylinker, they carried an extra 36 amino acid residues (~4.1 kDa) at the N-terminus.

The recombinant fragments A5, λ1a, λ2b and λ2c, as well as the full-length NuMA protein (Figure 1), were used in the cross-linking, CD and electron microscopic experiments described below. Chemical cross-linking experiments were used to determine the oligomeric state of the molecules. CD spectroscopy allowed an assessment of the secondary structure and showed that the central domain of NuMA indeed forms an extended α-helix. Electron microscopy monitored the ultrastructure of the NuMA molecule and its fragments.

*A5 fragment.* The A5 fragment covers amino acid residues 199–432 of NuMA. It includes the C-terminal part of the putative globular head (amino acids 199–215) and the amino terminal part of the putative helix (amino acids 216–432, Figures 1 and 3). After induction with isopropyl-thiogalactoside (IPTG) a 31 kDa polypeptide was expressed at high levels in *E.coli* (JM109) carrying the pRSET-NuMA 199–432 plasmid (Figure 3B, lane 1). Most of the A5 fragment was soluble when cells were sonicated in Tween-containing buffer. It was purified by metal chelate affinity chromatography on a Ni–NTA resin followed either by HPLC on a PLRP-S column or by chromatography on a phenylsuperose column. The second purification step provided a homogeneous protein (see Figure 3B, lane 2). The single band of the expected molecular weight seen in SDS–PAGE reacted positively in immunoblots with the SPN-3 antibody (Figure 3B, lane 3).

Chemical cross-linking experiments were used to determine the oligomeric state of the A5 fragment. The results of such experiments with low concentrations of glutaraldehyde were monitored by SDS–PAGE. Figure 5A shows that increasing concentrations of glutaraldehyde (0.001–0.4%) diminished the normal A5 band at 31 kDa and gave rise to a band with an apparent molecular mass of ~64 kDa, corresponding to a dimer. Similar experiments with disuccinimidyl tartrate (DST) and ethyleneglycol bis(succinimidyl succinate) (EGS) also showed that increasing cross-linker concentrations result in the appearance of a dimer band and a corresponding loss of the band in the monomer position. No additional bands at higher molecular masses were observed. Thus the native A5 fragment behaved as a dimer.

The CD spectrum of A5 in 80 mM phosphate buffer showed a substantial negative ellipticity at around 208 and 222 nm, consistent with a high α-helical content (Figure 6B). Electron micrographs of a glycerol sprayed/metal-shadowed A5 preparation documented rod-shaped molecules (Figure 7A) with an average length of 33 ± 4 nm (Table III) and a thickness of ~2–3 nm. Parallel experiments using the tetrameric rod of the intermediate filament protein desmin, which is around 48 nm in length (Potschka *et al.*, 1990), confirmed that the A5 molecule is appreciably shorter than the desmin rod (data not shown).

*λ1a fragment.* NuMA bp 157–2709, corresponding to amino acids 1–851 (see Figure 1), were expressed in *E.coli*, again using the pRSET vector. The λ1a fragment covers the entire head domain (residues 1–215) and the N-terminal 43% (residues 216–851) of the putative helical domain. SDS–PAGE showed that after induction with IPTG a major new band was present at ~100 kDa (Figure 5B, lanes 1 and 2). This reacted on immunoblots with the NuMA monoclonal antibody SPN-3 (not shown). The recombinant and His-tagged NuMA derivative, which was soluble in lysis buffer (Figure 5B, lane 3), was isolated by metal chelate chromatography (Figure 5B, lanes 7 and 8). Additional minor protein contaminants were removed by gel filtration on a Superdex 200 column (Figure 5C, lane 13). On a calibrated column the λ1a protein eluted prior to the position of the globular thyroglobulin (670 kDa). This early elution position suggests a long rod-like molecule.

The results of chemical cross-linking experiments with DST and EGS monitored by SDS–PAGE are shown in Figure 5C. In the absence of cross-linker (lane 13) fragment λ1a appeared as a single band with the expected molecular mass of the monomer, i.e. 101 kDa. After reaction of λ1a with DST at 37°C for 30 min the monomer band gradually disappeared (lanes 1–6) and a band of ~200 kDa was seen. Cross-linking of λ1a with EGS under the same conditions showed a dimer band even at the lowest concentration of cross-linker used (10 μg/ml). The CD spectrum of λ1a in phosphate-buffered saline showed the characteristic features of α-helices, with minima at 208 and 222 nm and a maximum at 195 nm (Figure 6C). Using the approximation method of Greenfield and Fasman (1969) at 208 nm we calculated an α-helix content of 67%. Based on the sequence of pRSET NuMA 1–851, the presumptive α-helical residues (positions 216–851) account for 72% of the molecule.

Electron microscopy of low angle rotary shadowed λ1a molecules showed thin rods with a small globular 'head' portion at one end (Figure 7B). The rod is 92 ± 9 nm in length (Table III), while the head has a diameter of ~14.1 nm (±1.5 nm). The approximately 3-fold length difference between λ1a and A5 corresponds to the increased length of the central rod domain covered by λ1a (Table III).

*λ2b fragment.* Fragment λ2b covers residues 670–1700 of the NuMA protein. It includes the C-terminal 69% of the putative α-helical rod region and stops at the presumptive

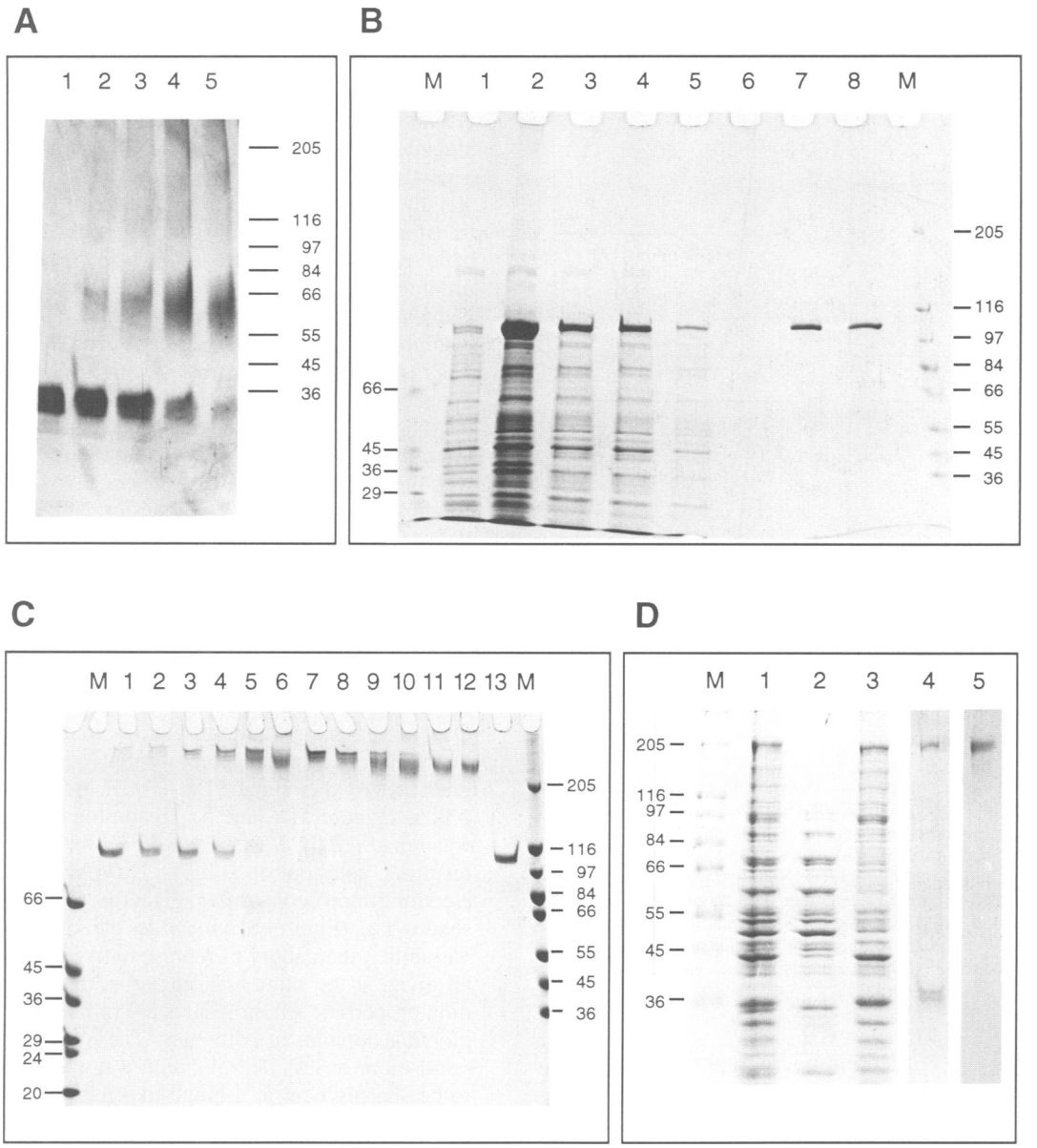


**Fig. 5.** Characterization and cross-linking studies of NuMA recombinant fragments. (**A**) Cross-linking of the A5 fragment, assayed by SDS–PAGE on silver stained 4–12% gradient gels. Lanes 1–5 correspond to glutaraldehyde concentrations of 0.001, 0.005, 0.01, 0.02 and 0.04% respectively. At the lowest concentration of glutaraldehyde the A5 fragment showed an apparent molecular weight of ~30 kDa. As the amount of cross-linker was increased, increasing amounts of A5 appeared in the dimer position (~60 kDa). At the highest concentration of cross-linker almost all the A5 is in the dimer position. (**B**) Expression and purification of the λ1a recombinant fragment assayed by SDS–PAGE on Coomassie blue stained 4–12% gradient gels. Lane 1, extract before induction with IPTG; lane 2, extract 4 h after induction; lane 3, lysate applied to Ni–NTA resin; lane 4, flow through; lane 5, first wash; lane 6, second wash; lanes 7 and 8, fractions eluted from the Ni–NTA resin with buffer containing 200 mM imidazole. The λ1a fragment has a molecular mass of ~100 kDa (lanes 7 and 8), which compares well with the molecular weight calculated from the sequence (101 kDa). (**C**) Cross-linking of the λ1a fragment assayed by SDS–PAGE on Coomassie blue stained 4–12% gradient gels. Lanes 1–6 correspond to DST concentrations of 10, 50, 100, 200, 500 and 1000 μg/ml; lanes 7–12 to similar EGS concentrations. Lane 13 is λ1a without cross-linker and served as control. Cross-linking with either DST or EGS resulted in dimer formation. Note that this process was already nearly quantitative at the lowest EGS concentration. (**D**) Expression and purification of full-length recombinant NuMA. Lane 1, culture 4 h after induction; lane 2, cell lysate with Tween, soluble part; lane 3, pellet of lysate solubilized with 8 M urea; lane 4, NuMA after gel filtration on a TSK 6000 column in 8 M urea; lane 5, NuMA after Mono Q anion exchange chromatography in 8 M urea. M, marker proteins with molecular weights shown on the left.

boundary between the rod and tail domains (see Figure 1). It was also expressed recombinantly in *E.coli*. IPTG treatment induced a polypeptide with a molecular mass of 122 kDa in SDS–PAGE. Gels of the lysate showed that λ2b was expressed to a lesser extent than λ1a. The soluble λ2b fragment was purified in the same manner as λ1a using an Ni–NTA resin as the first step and gel filtration on Superdex 200 as the second step. Such material provided a single band in SDS–PAGE (not shown).

The CD spectrum of fragment λ2b showed a substantial negative ellipticity at 208 and 222 nm, consistent with a high α-helical content (Figure 6D). Using the protein concentration obtained by quantitative amino acid analysis we calculated the α-helical content of the λ2b fusion

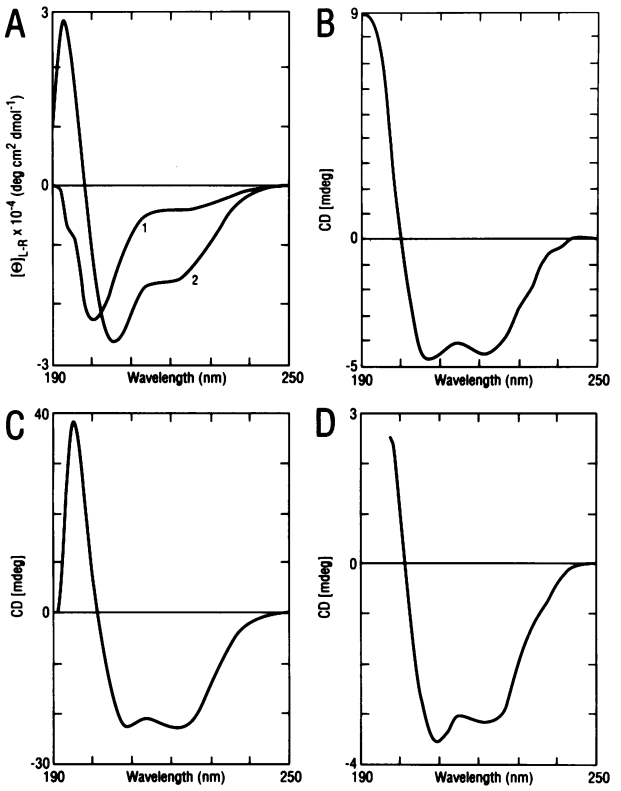


**Fig. 6.** Circular dichroism spectra. (**A**) Synthetic peptide 2, which includes the SPN-3 epitope (see Table II) in PBS (curve 1) and in PBS containing 50% trifluoroethanol (curve 2). Concentration 0.2 mg/ml. (**B**) NuMA fragment A5 in 80 mM potassium phosphate buffer, pH 7.0. Concentration ~200 μg/ml. (**C**) NuMA fragment λ1a in PBS with 0.1 mM dithiothreitol. Concentration 116 μg/ml. (**D**) Fragment λ2b in PBS with 0.1 mM dithiothreitol. Concentration 13 μg/ml. (A) Expressed as the molar mean residue ellipticity, (B–D) as millidegrees. The three NuMA fragments A5, λ1a and λ2b (B–D) show typical α-helical spectra.

protein to be ~90%. Electron micrographs of the glycerol sprayed/metal shadowed λ2b fragment again showed rod-shaped molecules (Figure 7C) with an average length of 136 ± 13 nm (Table III) and a thickness of ~2–3 nm. No globular portions were detected.

*λ2c fragment.* Fragment λ2c spans residues 1701–2115 of the NuMA protein. Therefore it does not include any of the proposed helical region and corresponds instead to the C-terminal 'tail' domain, which is thought to be globular (Compton *et al.*, 1992; Yang *et al.*, 1992; see also Figure 1). After induction with IPTG and cell lysis with Tween, the λ2c fragment was insoluble. It was solubilized with 8 M urea buffer containing 10 mM 2-mercaptoethanol and purified under denaturing conditions on the Ni–NTA resin. Subsequent dialysis against phosphate-buffered saline containing 2-mercaptoethanol led to renaturation of the λ2c fragment. When subjected to gel filtration on a standardized Superdex 200 column it eluted approximately in the position of ovalbumin (molecular mass 44 kDa). Since the calculated molecular mass of λ2c is ~49 kDa, the elution profile suggested a globular structure. SDS–PAGE of λ2c purified through Superdex showed a single polypeptide band. Electron microscopy of the glycerol sprayed/metal shadowed λ2c fragment revealed numerous globular structures and no rod-shaped molecules were detected (Figure 7D). The globular structures have a diameter of ~14.7 ± 1.4 nm.

*Full-length recombinant NuMA.* The full-length NuMA cDNA clone covering amino acids 1–2115 (Figure 1) was cloned into pRSET and expressed in *E.coli*. After induction a new polypeptide band appeared in the high molecular weight range (240 kDa) in the total cell lysate of bacteria transformed with the construct (Figure 5D, lane 1). This band reacted as expected with the SPN-3 antibody in immunoblots. Expression of the full-length recombinant NuMA protein was relatively low. The protein was insoluble when the cells were lysed with Tween (lane 2). The insoluble pellet was treated with 8 M urea to solubilize the recombinant protein (lane 3). It was not retained by the Ni–NTA resin and was found instead in the flow through fractions of the affinity matrix. The NuMA protein was therefore purified in 8 M urea using a gel filtration column (TSK 6000 PW or Superdex 200) as the first step. Recombinant NuMA eluted in the first fractions absorbing UV light (Figure 5D, lane 4). SDS–PAGE showed that a polypeptide of ~40 kDa was the major contaminant at this purification stage. N-Terminal sequencing identified this polypeptide as the *E.coli* membrane protein ompC (Mizuno *et al.*, 1983). The NuMA-containing fractions from the gel filtration column were pooled and applied to a Mono Q anion exchange column equilibrated with buffer 8 M in urea. NuMA protein free of ompC was eluted by a salt gradient. At this stage SDS–PAGE indicated a purity of >90% (Figure 5D, lane 5). Recombinant NuMA protein was renatured by dialysis against buffer without urea. The resulting solution of soluble NuMA was analysed by electron microscopy after glycerol spraying and metal shadowing (Figure 8). In spite of some ultrastructural variability, the gallery of representative NuMA molecules, all given at the same magnification, display several common properties. All molecules are rod-shaped and all have globular domains at both ends. The rods of the molecules seem more or less flexible, with a few of them appearing to be sharply bent at a hinge-like region near the middle of the molecule. The overall length of the rod is 207 ± 20 nm (Table III).

## Discussion

### *Molecular properties*

We have expressed and purified the full-length human NuMA protein and four fragments in *E.coli*. Under our expression conditions several recombinant fragments covering the central rod domain (A5, λ1a and λ2b) could be purified as native and soluble proteins. In contrast, the C-terminal globular domain (λ2c) and the full-length molecule were insoluble and were therefore purified as denatured proteins in 8 M urea. Subsequent dialysis to remove the urea led to soluble proteins. CD spectra showed that fragments from the putative rod domain (residues 216–1700) were characterized by typical α-helical spectra. For the λ2b fragment, which covers residues 670–1700, we obtained an α-helical content of at least 90%. The λ1a fragment, which covers residues 1–851, had 67% α-helix. If the globular N-terminal head domain (residues 1–215) is subtracted from the λ1a fragment (residues 1–851), the helix content of the λ1a

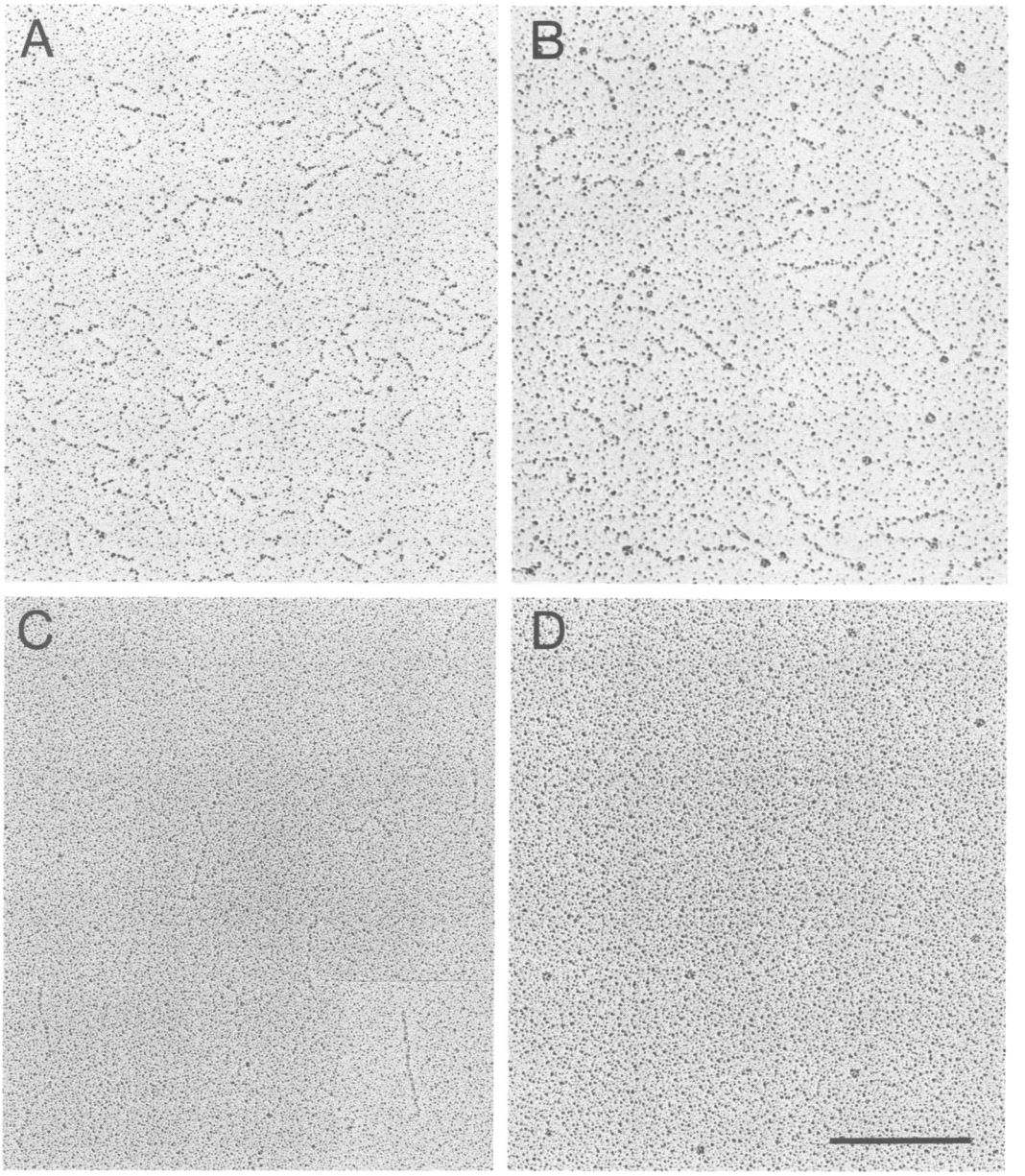


**Fig. 7.** Electron micrographs of recombinant NuMA fragments obtained after rotary shadowing. (**A**) A5 fragment. Note the thin rods (length ~30 nm). (**B**) λ1a fragment. Note the thin rods (length ~90 nm) and the small globular head at one end of the rod. (**C**) λ2b fragment. Note the thin rod (length ~140 nm) and the absence of globular structures. (**D**) λ2c fragment. Only globular structures are visible. Bar 200 nm for all micrographs.

**Table III.** Comparison of the measured rod length (nm) of NuMA and its derivatives and the lengths calculated from the α-helical segments

| Fragment | NuMA protein residues | α-helical residues | Coiled-coil residues | Calculated rod length | Measured rod length |
|---|---|---|---|---|---|
| A5 | 199–432 | 216–432 | 217 | 32 | 33 ± 4 |
| λ1a | 1–851 | 216–851 | 636 | 94 | 92 ± 9 |
| λ2b | 670–1700 | 670–1700 | 1031 | 153 | 136 ± 13 |
| λ2c | 1701–2115 | – | – | – | – |
| NuMA | 1–2115 | 216–1700 | 1485 | 221 | 207 ± 20 |

putative rod portion can be as high as 93%. From the protein sequence of NuMA (Compton *et al.*, 1992; Yang *et al.*, 1992) one can expect a very high degree of helicity, although the presence of several proline residues, occurring either singly or in tandem, indicate the existence of six short non-helical spacers (6, 7, 19, 7, 5 and 6 amino acids long) which interrupt the α-helix (Yang *et al.*, 1992; see Figure 2). A more detailed analysis of the rod sequence indicates 12 additional discontinuities in the phasing of the heptad substructure which do not involve prolines. All are likely to have some effect on the ability of the rod to bend, kink or otherwise allow some deformation to occur. Thus the rod region may consist of 19 distinct α-helical segments (Parry, 1994). Consistent with this, our CD

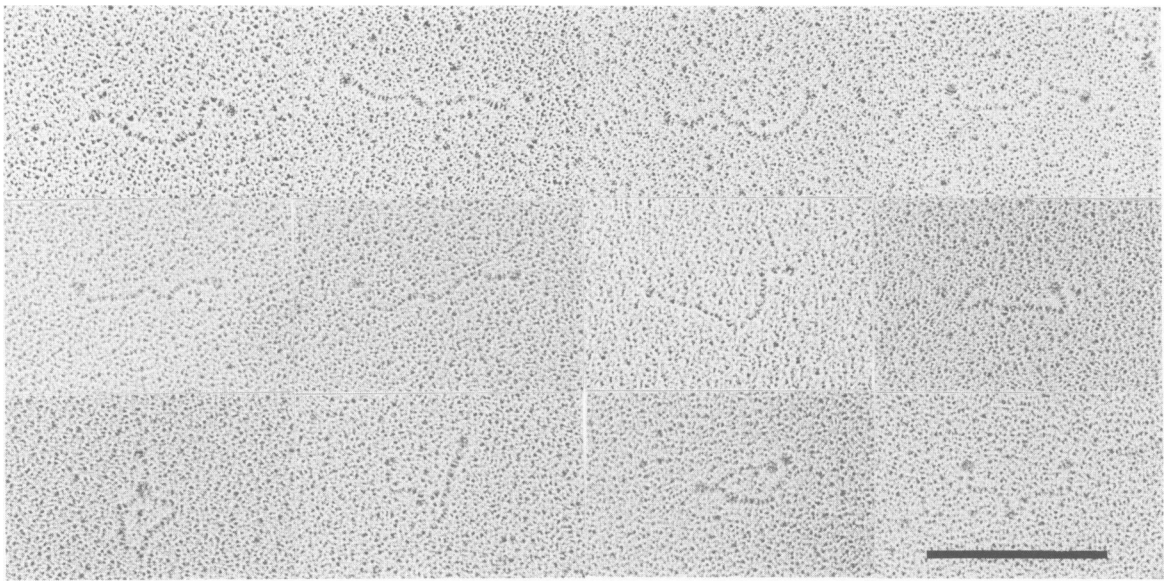

**Fig. 8.** Gallery of recombinant full-length NuMA molecules after low angle rotary shadowing. Globular domains are seen at both ends of each molecule. Some molecules are bent. Bar 200 nm.

spectra show that the rod domain must be considered as a segmented coiled-coil which does not reach 100% α-helix.

To decide whether the putative coiled-coil formed by NuMA is double- or triple-stranded (Cohen and Parry, 1990) we chemically cross-linked the A5 and λ1a fragment with glutaraldehyde, DST and EGS. The dimeric state of the molecules, documented by SDS–PAGE, shows that NuMA forms a double-stranded coiled-coil. Since A5 and λ1a are both from the N-terminal side of the rod, the two α-helices forming the coiled-coil of the rod domain must be arranged in parallel. This view is directly supported by the electron microscopical results on NuMA and its fragments. They appear as long thin rods. Rods with a globular structure at one end are seen with λ1a, which retains the N-terminal head domain, while λ2b, which lacks both terminal domains, appears as a rod with no associated globular structures. Full-length NuMA molecules, in contrast, show a long rod with globular structures at both ends. The combined results support the view of a double-stranded coiled-coil in which the participating α-helices are arranged in parallel without a major stagger. The C-terminal domain of 415 residues (λ2c) purified in 8 M urea stays soluble after removal of urea. Such material behaves as a monomer in gel filtration, where it elutes in the position of ovalbumin (molecular mass 43 kDa), and electron microscopy shows globular particles. Thus the domain can to some extent refold from urea, but whether the renaturation process is perfect is not yet known.

Correlations between the length of rod domains, measured by direct observation, and the length of predicted α-helical segments have been made for a number of coiled-coil proteins, including myosin (Stewart and Edwards, 1984), paramyosin (Cohen *et al.*, 1987), cytoplasmic intermediate filament proteins (Potschka *et al.*, 1990) and nuclear lamins (Heins and Aebi, 1994). A similar correlation is provided for NuMA in Table III, where the values measured for the different rod constructs described in this study are compared with the lengths derived from the sequence using secondary structure rules and a length of 1.485 Å per helical residue. Examination of Table III shows that the calculated lengths are in surprisingly good agreement with the measured lengths.

NuMA has a documented coiled-coil of 207 nm. This value clearly exceeds the myosin coiled-coil of 154 nm (Stewart and Edwards, 1984) and is, indeed, the longest coiled-coil so far reported.

### *Does NuMA form higher order structures?*

The NuMA protein sequence shares a certain topographical similarity with the sequences of the structural proteins of the cytoplasmic intermediate filaments and of the nuclear lamina (Fuchs and Weber, 1994). In both cases a central coiled-coil forming domain is flanked by non-helical terminal domains and both cytoplasmic intermediate filament proteins and nuclear lamins can form higher order filaments *in vitro*. Indeed, because of these similarities in structure and because in interphase NuMA is found in the nuclear matrix, several authors have suggested that NuMA may be a structural component of the nucleoskeleton (Lydersen and Pettijohn, 1980; Kallajoki *et al.*, 1991, 1993; Yang and Snyder, 1992). Nuclear filaments have been visualized under some conditions in the electron microscope, although their significance is controversial (Cook, 1988). Filaments, obtained after lysing cells encapsulated in agarose microbeads, nuclease digestion and electroelution of the DNA, have a diameter of around 10 nm, with an axial repeat of 23 nm (Jackson and Cook, 1988). Alternatively, smooth 9–13 nm nuclear core filaments have been reported after extraction with 0.25 M ammonium sulfate and high salt gradients (He *et al.*, 1990). Indeed, Zeng *et al.* (1994) have shown immunoelectron micrographs of a gold-labelled NuMA antibody bound to nuclear filaments prepared by the method of He *et al.* (1990). Although this data again raises the question of whether purified recombinant NuMA can polymerize *in vitro* to form filaments, thus far we have no evidence that this is the case. Under our *in vitro* conditions recombinant NuMA purified from *E.coli* neither forms higher order

structures nor assembles into filaments, but stays instead as a double-stranded coiled-coil.

There could be several reasons why our *in vitro* assembly system may not be optimal. (i) The buffer system may be suboptimal for assembly; (ii) renaturation of the globular head and tail domains of NuMA from 8 M urea may be incomplete; (iii) the recombinant NuMA molecules contain 36 additional residues in front of the head domain due to the cloning system used and this tag could interfere with assembly; (iv) putative higher order structure may require post-translational modification(s) and/or processing which is not provided by recombinant protein expression in *E.coli*. Some of these potential shortcomings can be overcome in the future. Thus a highly specific cleavage site could be used to remove the entire tag from the purified protein by specific proteolysis. Alternatively, NuMA could be expressed with the bacculovirus system in insect cells to see whether eukaryotic post-translational modifications are important. Currently it is more difficult to see how renaturation of the terminal domains could be improved, since recombinant NuMA is insoluble in normal buffer and thus has to be purified in 8 M urea. However, one possibility could be to use chaperones during the renaturation process.

Alternatively, NuMA may indeed not be able to form filaments on its own. Thus a detailed analysis of the distribution of positive and negative charges along the helical arrays reveals a lack of the typical periodicities found in corresponding regions of filament forming molecules such as myosin II, paramyosin and the structural proteins of intermediate filaments, where filament forming ability is based on lateral and longitudinal interactions of coiled-coils (Parry, 1994). While these observations, as well as our current results, provide no support for NuMA as a major constituent of nuclear filaments, they leave open the possibility that NuMA may form higher order complexes containing several dimeric molecules or that NuMA may form specific complexes with other cellular proteins. Indeed, the established functional significance of NuMA in the mitotic spindle (Kallajoki *et al.*, 1991, 1993; Yang and Snyder, 1992) and its insolubility in the interphase nuclear matrix (Lyderson and Pettijohn, 1980; Kallajoki *et al.*, 1991) directly argue for binding to other cellular components. This problem could be approached by use of the two-hybrid system (Chien *et al.*, 1991). This may be a very useful approach, since NuMA may have, parallel to its different locations within the cell, different binding partners during interphase in the nucleus and during mitosis at the spindle poles.

### *Epitope location*

The immunodominant epitopes of NuMA appear to be concentrated in the long central rod domain of the protein. Thus four of the five monoclonal antibodies mapped in this study have their epitopes in the rod, as do the 1H1, 1F1, 2D3 and 2E4 monoclonal antibodies, where the epitope location has been approximately mapped by others (Compton *et al.*, 1992). Only the SPN-4 epitope, mapped to the region between NuMA residues 199 and 216, lies at the C-terminal end of the globular head domain just prior to the α-helical rod.

The epitope of the SPN-3 NuMA monoclonal antibody was of particular interest because this antibody inhibited mitosis and led to micronucleation when injected into cells, while the SPN-1, -2, -4 and -5 antibodies did not (Kallajoki *et al.*, 1991). Use of several recombinant NuMA clones and subclones located the SPN-3 epitope to the N-terminal part of the rod domain (residues 247–279) and a set of synthetic peptides refined the analysis. The SPN-3 epitope is a linear epitope which arises from the tridecapeptide covering residues 255–267 of the human NuMA polypeptide. This sequence directly preceeds the first non-helical spacer of the rod domain (Figure 2). Mutant peptides with single amino acid replacements identified several positions of the epitope with very strict sequence requirements. Interestingly, neither Asp259 nor Arg260 tolerate the highly conservative replacement by Glu or Lys respectively (Figure 4). This high sequence dependence may contribute to the relatively limited cross-species reactivity of the SPN-3 antibody (Kallajoki *et al.*, 1991) and may become more obvious once NuMA sequences from additional species become available.

Our results do not explain why SPN-3 was the only monoclonal antibody of those tested which inhibited mitosis after microinjection. McIntosh and Koonce (1989) have compiled a list of spindle components and commented that a monoclonal antibody affected microinjection in only very few cases. Thus it seems that various monoclonal antibodies either do not find access to their epitope within the living cell or do not have a sufficiently high affinity to stay bound at the epitope. Alternatively, occupation of the epitope by the antibody may not necessarily exert a perturbing effect on mitosis. In this respect we note that an antibody molecule can cover on its antigen some 3 nm in length, which on a coiled-coil would correspond to some 20 α-helical residues (Colman *et al.*, 1987).

Effects similar to those first demonstrated for the SPN-3 NuMA antibody in microinjection experiments, i.e. mitotic arrest with perturbed mitotic spindle formation and formation of micronuclei (Kallajoki *et al.*, 1991), have also been observed by others. Thus injection of a rabbit antibody directed against an 85 kDa recombinant fragment of the NuMA rod (GST:2) into interphase or prophase monkey CV-1 cells blocked formation of the mitotic spindle, while injection of the same antibody into metaphase cells caused the preformed spindle to collapse (Yang and Snyder, 1992). Interestingly, the GST:2 fragment corresponds approximately to the C-terminal two thirds of segment 3 and segment 4 and therefore does not contain the SPN-3 epitope site. In addition, transfection of NuMA constructs lacking amino acids 19–208 results in BHK-21 cells that fail to complete cytokinesis and form micronuclei in the subsequent interphase. In contrast, NuMA constructs lacking the globular tail domain result in cells that complete mitosis but then form micronuclei in each daughter cell (Compton *et al.*, 1992). Interestingly, the defect in the hamster tsBN2 cell line, which forms micronuclei at the restrictive temperature, can be rescued by transfection with human NuMA (Compton and Cleveland, 1993). Taken together, these results suggest that binding of the SPN-3 antibody to its epitope or, alternatively, certain deletions and truncations of NuMA result in major perturbations in spindle function and in nuclear reformation in the subsequent interphase. The molecular basis for these effects may become more obvious once NuMA binding proteins are identified in the future.

## Materials and methods

### Immunoscreening

The screen was performed as described for a lamin cDNA clone (Stick, 1988) using two HeLa cell cDNA libraries, one in the Uni-ZAP XR vector and the other in the λ ZAP II vector (Stratagene, Heidelberg, Germany). A total of 1 800 000 clones were screened with a mixture of the hybridoma supernatants from six previously characterized antibodies to the SPN/NuMA antigen, i.e. SPN-1 to -5 and SPN-7 (Kallajoki *et al.*, 1991), after induction of the β-galactosidase fusion proteins by 10 mM IPTG (Biomol, Hercules, CA). The antibody incubation was carried out with a mixture of supernatants from the six SPN/NuMA antibodies, to which 0.05% Tween-20 and 0.1% pig haemoglobin were added. Antibody-reactive clones were visualized using as second antibody alkaline phosphatase-conjugated goat anti-mouse antibodies (Dianova, Hamburg Germany; 1:2 000 in TBS-T buffer) and as developing solution 0.33 mg/ml nitrobluetetrazolium (NBT) and 0.2 mg/ml bromochloro-indolyl phosphate (BCIP; Sigma, St Louis, MO) in 0.1 M $Na_2CO_3$, pH 10.2. Positive plaques were picked, replated at lower density and rescreened. This procedure was repeated until all phages on the plate were immunoreactive with the antibody mixture. Reactivity with each individual NuMA monoclonal antibody was subsequently analysed.

The screening yielded a total of seven immunoreactive clones, five from the λ ZAP II library (λ1–λ5) and two from the Uni-ZAP XR library (Uni-1 and -2). Bluescript SK phagemids containing the cloned cDNA insert of the immunoreactive phages were excised by co-infection with the R408 helper phage according to the manufacturer's protocol (Stratagene) and purified by standard protocols. Sequencing was performed by the dideoxy chain termination reaction according to Sanger *et al.* (1977). T3 and T7 primers, as well as specific primers derived from the NuMA sequence of Yang and Snyder (1992), were employed.

### Expression of β-galactosidase fusion proteins

λ phages were diluted to a concentration sufficient for plaques to form a nearly confluent monolayer after 8 h at 42°C. IPTG (50 mM) was then added and the plates incubated for a further 3 h at 37°C. SDS sample buffer was then added and the samples harvested, heated to 100°C and used for SDS–PAGE.

### Construction of full-length and partial NuMA cDNAs

Since the immunoscreen of the cDNA libraries yielded only partial NuMA cDNAs, full-length NuMA cDNA was constructed from the two overlapping clones λ1 and λ2 (Figure 1). These spanned nucleotides 65–2710 and 2163–7145 respectively (Yang *et al.*, 1992) and thus covered the entire coding region. A unique *Bst*EII site was present in both clones at bp 2292 and allowed ligation between λ1 and λ2 after digestion with *Bst*EII. To eliminate non-translated regions of the NuMA sequence from λ1, PCR was used to amplify the portion of the λ1 cDNA covering nucleotides 157–2709. This new construct, λ1a, started directly with the ATG initiating codon and contained a unique *Bam*HI site immediately upstream from the ATG. PCR was used in a similar manner to amplify the portion of the λ2 cDNA covering nucleotides 2164–6501. This new construct, λ2a, ended with the TAA stop codon and contained an *Eco*RI site immediately following this codon. λ1a was then digested with *Bam*HI and *Bst*EII and λ2a with *Eco*RI and *Bst*EII. The resulting fragments were ligated at the *Bst*EII site and introduced into the *Bam*HI/*Eco*RI linearized pRSETA expression vector (Invitrogen, San Diego, CA). This expression vector contains a T7 promoter, a metal binding domain (His-tag) and a gene 10 sequence, allowing the identification of recombinant proteins with an antibody recognizing the T7 tag (Kroll *et al.*, 1993). Thus the N-terminal sequences of the NuMA derivatives are preceeded by 36 residues encoded by the expression vector.

Additional truncated mutants of λ1 (λ1b, λ1c and λ1d) and the λ2 clone (λ2b and λ2c) (see Figure 1) were constructed in a similar manner using λ1 or λ2 as templates. PCR used Vent polymerase (New England Biolabs, Beverly, MA), which ensured high fidelity base incorporation due to its 3′→5′ proof-reading exonuclease activity. Primer pairs were as follows: λ1a (33, 36), λ1b (33, 20), λ1c (27, 36), λ1d (27, 37), λ2a (34, 38), λ2b (34, 39), λ2c (35, 38) (see Table IV, where the numbers indicate the nucleotide positions of NuMA taken from the cDNA sequence of Yang *et al.*, 1992). Some PCR amplified products were first subcloned in the pCRII vector (Invitrogen) and released by cleavage with *Bam*HI/*Hin*dIII or with *Bam*HI/*Eco*RI digestion before ligation into the appropriate restriction site in the pRSETA vector.

For mapping of the SPN-3 epitope a series of NuMA pRSET expression plasmids was generated by amplifying different regions of NuMA cDNA from the Uni-1 clone plasmid DNA using Taq DNA polymerase (Promega, Madison WI). Primer pairs were as follows: A1 (17, 20), A2 (18, 21), A3 (19, 22), A4 (17, 21), A5 (18, 22), N1 (18, 30), N2 (27, 31), N3 (28, 32), N4 (29, 21), N5 (18, 31), N6 (28, 21), N7 (27, 32) (see Table IV). All final products were cloned in-frame with the fusion protein part of the pRSET vector by an appropriate choice of the 5′-end primers.

### Overexpression of fusion proteins

Two millilitres of SOB containing ampicillin at 50 μg/ml were inoculated with a single recombinant *E.coli* JM109 colony harbouring the appropriate plasmid and grown overnight at 37°C with shaking. Aliquots (0.8 ml) of this overnight culture was used to inoculate 200 ml of SOB medium containing 50 μg/ml ampicillin. Cultures were then grown with shaking at 37°C until they reached an optical density at 600 nm of 0.3. Overexpression of the recombinant protein was initiated by adding 1 mM IPTG. One hour later cells were infected with M13/T7 phage at a multiplicity of infection of 5 plaque-forming units/cell, incubated for an additional 4 h to permit maximal expression of fusion proteins and harvested by centrifugation (4000 *g* for 20 min).

### Purification of recombinant proteins

Cells from three 200 ml cultures were resuspended in 10 ml lysis buffer (50 mM potassium phosphate, pH 7.9, 500 mM KCl, 10 mM 2-mercaptoethanol, 1 mM phenylmethylsulfonyl fluoride, 0.2% Tween 20) and sonicated. The lysate was clarified by centrifugation at 10 000 *g* for 15 min.

In the case of NuMA derivatives which were soluble in lysis buffer the supernatant was applied directly to Ni–NTA resin (Quiagen, Chatsworth, CA), packed in a chromatography column and equilibrated in lysis buffer. The flow through was usually re-applied to the column and a flow rate of 2–5 ml/h was used. The resin was washed with lysis buffer. The second wash was with lysis buffer, pH 6.0, containing up to 20 mM imidazole. Proteins were eluted in the same buffer using a 20–500 mM imidazole gradient.

For NuMA derivatives insoluble in lysis buffer the pellet was treated with urea buffer (8 M urea, 20 mM Tris–HCl, pH 7.9, 500 mM NaCl, 10 mM 2-mercaptoethanol). After sonication and centrifugation the supernatant was also fractionated by metal chelate affinity chromatography on Ni–NTA resin (Quiagen). The column was washed with urea buffer, followed by a second wash with urea buffer, pH 6.3, containing 5 mM imidazole. Proteins were eluted in the same buffer using a 5–500 mM imidazole gradient.

Fractions were monitored spectrophotometrically and analysed by SDS–PAGE. After identification of the fractions containing the recombinant protein, the proteins were further purified. Fusion protein N3 was purified by HPLC on a Vydac 214 TP52 column; fusion protein A5 was purified either by HPLC (PLRP-S column) or by a phenylsuperose column (50 mM MES, pH 6, 1 mM EDTA, 0.3 mM dithiothreitol), using a gradient of 1–0 M $(NH_4)_2SO_4$; fusion proteins λ1a and λ2b were purified by gel filtration on Superdex 200 under native conditions; fusion protein λ2c and the full-length NuMA protein (FL) were purified by gel filtration in the presence of 8 M urea on Superdex 200 (Pharmacia) or TSK 6000 PW (Toso Haas). Full-length NuMA was further purified by Mono-Q chromatography in the presence of 8 M urea.

### Cross-linking

Fragment A5, purified by HPLC at a concentration of 30–40 μg/ml, was dialysed for 12 h at 4°C against phosphate-buffered saline (PBS) containing 2.5 mM dithioerythritol. Glutaraldehyde (Serva, Heidelberg, Germany) was added to aliquots such that final concentrations ranged from 0.001 to 0.04%. Samples were incubated for 30 min at 14°C. The cross-linking reactions were terminated by addition of one half volume of the same buffer containing 2 M glycine. Cross-linked samples were resolved by SDS–PAGE using 4–12% gradient gels.

The fusion protein λ1a was dialysed against 50 mM triethanolamine–HCl, pH 8.0, containing 0.17 M NaCl and 1 mM 2-mercaptoethanol. The protein concentration was adjusted to ~0.1 mg/ml. EGS or DST (both from Pierce) were dissolved in dimethylsulfoxide at 7.5 mg/ml. Cross-linker was added to the protein solution to final concentrations ranging from 0 to 1 mg/ml. Cross-linking was for 30 min at 37°C. Reactions were stopped by adding ethanolamine–HCl, pH 8.0, to a final concentration of 0.1 M for 15 min at room temperature. The EGS or DST cross-linked material was directly applied to SDS–PAGE.

### Circular dichroism

The A5 fragment was dialysed against 80 mM potassium phosphate, pH 7.0, while the other purified fusion proteins were dialysed against

**Table IV.** Sequence of primers used for PCR amplification

| PCR primer | Sequence 5′→3′ | Restriction enzyme site | | Position in NuMA-sequence | |
|---|---|---|---|---|---|
| | | | | 5′ | 3′ |
| 17 | GCATGGATCCAAAATTCAGGCTGAGTTGGCTGTC | *Bam*HI | s | 520 | 543 |
| 18 | GCATGGATCCGGTTCTCCAGCTTCTCCCATGG | *Bam*HI | s | 751 | 772 |
| 19 | GCATGGATCCCTTACCATGCGGCTGCATGAAACC | *Bam*HI | s | 1018 | 1041 |
| 20 | GGCATAAGCTT**TTA**CATCTGGAACTGTGGGGTCTGCAG | *Hin*dIII | as | 804 | 781 |
| 21 | GGCATAAGCTT**TTA**CTTCTCTGTCTTCAGGTCCTGGC | *Hin*dIII | as | 1074 | 1052 |
| 22 | GGCATAAGCTT**TTA**GAGCTGTGTGTTGTTTGCAGCAAG | *Hin*dIII | as | 1452 | 1429 |
| 27 | GCATGGATCCATGAGACGGCTGAAGAAGCAGCTTGC | *Bam*HI | s | 802 | 827 |
| 28 | GCATGGATCCAAGGATGCACAGATAGCCATGATGC | *Bam*HI | s | 895 | 919 |
| 29 | GCATGGATCCGAGCCCAAGGAGCTTGAGGAGCTGC | *Bam*HI | s | 976 | 1000 |
| 30 | GGCATAAGCTT**TTA**ATCAGCAAGCTGCTTCTTCAGCCG | *Hin*dIII | as | 831 | 808 |
| 31 | GGCATAAGCTT**TTA**GGCTATCTGTGCATCCTTCTCGG | *Hin*dIII | as | 912 | 890 |
| 32 | GGCATAAGCTT**TTA**CTCAAGCTCCTTGGGCTCCAGTGG | *Hin*dIII | as | 993 | 970 |
| 33 | GCATGGATCCATGACACTCCACGCCACCCGGGGGGCTG | *Bam*HI | s | 157 | 184 |
| 34 | GCATGGATCCCAGGCCCAGGTTGCAGAGCTAGAGTTGC | *Bam*HI | s | 2164 | 2191 |
| 35 | GCATGGATCCCAGGTGGCAACTGATGCTTTAAAGAGCCG | *Bam*HI | s | 5257 | 5285 |
| 36 | GGCATAAGCTT**TTA**CTCCTGCAGCTCCTGGCGGGCCTTC | *Hin*dIII | as | 2709 | 2685 |
| 37 | GGCATAAGCTT**TTA**GGCCTCATGCTGTTCCTGGCGGGC | *Hin*dIII | as | 2163 | 2140 |
| 38 | GGCATGAATTC**TTA**GTGCTTTGCCTTGCCCTTGGCTCG | *Eco*RI | as | 6501 | 6478 |
| 39 | GGCATGAATTC**TTA**GAATTTGCCCAGGTCTCGAAGCTGC | *Eco*RI | as | 5256 | 5232 |

s, sense; as, antisense
The restriction enzyme site within the sequence is underlined, and the stop codon is shown in bold print.

PBS. Measurements were performed with a Jasco J-720 spectropolarimeter (Japan Spectroscopic Co. Ltd, Tokyo, Japan) using a cuvette with a 0.1 cm path length. Final protein concentrations were determined by quantitative amino acid analysis.

### *Electron microscopy*

Fragment A5 purified by HPLC was dialysed against 20 mM Tris–HCl, pH 7.4, 150 mM NaCl. Fragments λ1a and λ2b were dialysed after the gel filtration step (see above) against 50 mM potassium phosphate, 500 mM KCl. Fragment λ2c purified by gel filtration under denaturing conditions was dialysed against 20 mM Tris–HCl, 20 mM NaCl, 1 mM dithiothreitol, pH 7.2, for 4 h at room temperature on a nitrocellulose filter (0.025 μm; Millipore). The full-length NuMA protein obtained by anion exchange chromatography in 8 M urea was renatured by dialysis against 20 mM Tris–HCl, pH 7.2, 1 mM dithiothreitol on nitrocellulose filters.

Glycerol was added to the protein solutions to a final concentration of 50%. The protein solutions were then sprayed on to freshly cleaved mica flakes, which were subsequently dried under vacuum. Rotary shadowing with tantalum/tungsten or platinum was performed at an angle of 5° or 9° respectively using a modified Balzers apparatus followed by carbon shadowing at 90°. Replicas were floated off on a surface of distilled water and collected on copper grids (400 mesh, TAAB, Munich).

### *Gel filtration analysis*

Analytical gel filtration chromatography was performed using the SMART micro FPLC facility (Pharmacia, Uppsala, Sweden) and a Superdex 200 HR 10/30 gel filtration column (Pharmacia) equilibrated in PBS containing 1 mM dithiothreitol. Proteins were separated at a flow rate of 40 μl/min at room temperature. Elution profiles were monitored at 280 nm. The system was calibrated with molecular weight standards (Bio-Rad, Munich, Germany).

### *SDS gel electrophoresis and immunoblotting*

SDS–PAGE was performed in 0.5 mm thick slab gels containing 10% acrylamide. In some experiments gradient gels with 4–12% acrylamide or tricine gels with a spacer gel of 10%/3% and a separating gel of 16.5%/3% were used (Schägger and von Jagow, 1987). For immunoblotting, polypeptides separated by SDS–PAGE were transferred electrophoretically onto nitrocellulose membranes (Schleicher & Schuell). The transfer buffer contained 25 mM Tris–HCl, 190 mM glycine, 0.01% SDS, 20% methanol. The nitrocellulose strips were stained reversibly with Ponceau S. Blocking of the nitrocellulose membrane and subsequent immunological detection followed the protocol given in the section on immunoscreening. Peroxidase-conjugated second antibodies were detected with chloronaphthol or with diaminobenzidine.

### *Synthetic peptides and quantitative amino acid analysis*

Peptides were synthesized on an automated synthesizer (model 9050; Milligen) based on protection of the amino group with 9-fluorenyl methoxycarboxyl. Synthesis and deprotection followed the standard protocol of the manufacturer. Peptides were purified by HPLC on a preparative reverse-phase column (Vydac 218 Tp, 10 μm). Sequence identity was verified by automated gas phase sequencing on an Applied Biosystems gas phase sequenator (model A470) or a Knauer sequenator (model 810). Both instruments were equipped with an on-line phenylthiohydantoin amino acid analyser. The exact peptide concentrations were determined by quantitative amino acid analysis. After hydrolysis in propionic acid/HCl at 150°C for 1 h, amino acids were subjected to pre-column derivatization with phenylisothiocyanate (Bidlingmeyer *et al.*, 1984) and analysed on a HPLC reverse phase column. The peptide stocks were then adjusted to a concentration of 2 mM in PBS and stored at −20°C until use.

### *Coupling of peptides to ovalbumin*

Twenty five milligrams of ovalbumin (Sigma) in 1 ml PBS and 9 mg *m*-maleimidobenzoyl-*N*-hydroxysulfosuccinimide ester (Sulfo-MBS; Pierce, Rockford, IL) in 0.5 ml PBS were mixed and incubated with rotation for 30 min at room temperature. Uncoupled Sulfo-MBS was removed on a PD10-column equilibrated with 50 mM sodium phosphate buffer, pH 6. Usually ~2.5 ml of ovalbumin–Sulfo-MBS was obtained. Five milligrams of purified peptide in 4 ml PBS was mixed with 500 μl ovalbumin–Sulfo-MBS fraction from the PD10 column and 300 μl 0.5 M sodium phosphate buffer, pH 7.5. Incubation was for 3 h at room temperature on a rocking platform. The coupled peptides were either used directly in the dot blot assay or stored at −20°C.

### *Competitive ELISA*

The recombinant fusion protein λ1a was used as the antigen. It was diluted to a final concentration of 0.6 μg/ml with coating buffer (15 mM $Na_2CO_3$, 35 mM $NaHCO_3$). A 50 μl aliquot containing 30 ng λ1a protein was pipetted into each well of a 96-well microtitre plate (Immunolon F-Form; Dynatech, Denkendorf, Germany). Plates were incubated overnight at 4°C and then for 30 min at room temperature. The plates were washed three times with PBS, blocked for 2 h at 37°C with PBS containing 4% bovine serum albumin (BSA) and then washed three times with PBS. A dilution series was made for each peptide in PBS containing 1% BSA, so that end concentrations were between $10^{-7}$ and $10^{-3}$ M. These were preincubated with an equal volume of the SPN-3 monoclonal antibody (SPN-3 hybridoma supernatant diluted 1:100 in the same buffer) for 30 min at room temperature. The different peptide/antibody mixtures (50 μl) were pipetted into the microtitre plates containing λ1a and incubated for 1.5 h at 37°C. Subsequently the wells were washed three times with PBS and incubated for 1.5 h at 37°C with

the second antibody (peroxidase-conjugated rabbit anti-mouse diluted 1:400 in PBS containing 1% BSA; Dako, Klostrup, Denmark). The wells were washed again with PBS and 100 µl of freshly prepared developing solution were added [10 mg *o*-phenylene diamine dissolved in 25 ml of buffer (25 mM sodium citrate, 50 mM $Na_2HPO_4$, pH 5.0) to which 10 µl 30% $H_2O_2$ were added just before use] and incubation continued for 10 min at room temperature. The reaction was stopped with 2.5 M sulfuric acid and the optical density was measured at 490 nm using an ELISA reader (Dynatech, Model MR 700).

## Acknowledgements

We thank Dr Volker Gerke for advice on molecular cloning and for critical comments on the manuscript, Uwe Plessmann, Monika Dietrich and Heinz-Jürgen Dehne for expert technical help and Irene Gajewski for photographic assistance. This work was supported by a grant from the Deutsche Forschungsgemeinschaft (Os 70/2-2).

## References

Bidlingmeyer,B.B., Cohen,S.A. and Tarvin,T.L. (1984) Rapid analysis of amino acids using pre-column derivatization. *J. Chromatogr.*, **336**, 93–104.

Chien,C.-T., Bartel,P.L., Sternglanz,R. and Fields,S. (1991) The two-hybrid system: a method to identify and clone genes for proteins that interact with a protein of interest. *Proc. Natl Acad. Sci. USA*, **88**, 9578–9582.

Cohen,C. and Parry,D.A.D. (1990) α-Helical coiled coils and bundles: how to design an α-helical protein. *Protein Struct. Function Genet.*, **7**, 1–15.

Cohen,C., Lanar,D.E. and Parry,D.A.D. (1987) Amino acid sequence and structural repeats in schistosome paramyosin match those of myosin. *Biosci. Rep.*, **7**, 11–16.

Colman,P.M., Laver,W.G., Varghese,J.N., Baker,A.T., Tulloch,P.A., Air,G.M. and Webster,R.G. (1987) Three-dimensional structure of a complex of antibody with influenza virus neuraminidase. *Nature*, **326**, 358–363.

Compton,D.A. and Cleveland,D.W. (1993) NuMA is required for the proper completion of mitosis. *J. Cell Biol.*, **120**, 947–957.

Compton,D.A., Yen,T.J. and Cleveland,D.W. (1991) Identification of novel centromere/kinetochore-associated proteins using monoclonal antibodies generated against human mitotic chromosome scaffolds. *J. Cell Biol.*, **112**, 1083–1097.

Compton,D.A., Szilak,I. and Cleveland,D.W. (1992) Primary structure of NuMA, an intranuclear protein that defines a novel pathway for segregation of proteins at mitosis. *J. Cell Biol.*, **116**, 1395–1408.

Cook,P.R. (1988) The nucleoskeleton: artefact, passive framework or active site? *J. Cell Sci.*, **90**, 1–6.

Fuchs,E. and Weber,K. (1994) Intermediate filaments: structure, dynamics, function and disease. *Annu. Rev. Biochem.*, **63**, 345–382.

Greenfield,N. and Fasman,G.D. (1969) Computed circular dichroism spectra for the evaluation of protein conformation. *Biochemistry*, **8**, 4108–4116.

He,D., Nickerson,J.A. and Penman,S. (1990) Core filaments of the nuclear matrix. *J. Cell Biol.*, **110**, 569–580.

Heins,S. and Aebi,U. (1994) Making heads and tails of intermediate filament assembly, dynamics and networks. *Curr. Opin. Cell Biol.*, **6**, 25–33.

Jackson,D.A. and Cook,P.R. (1988) Visualization of a filamentous nucleoskeleton with a 23 nm axial repeat. *EMBO J.*, **7**, 3667–3677.

Kallajoki,M., Weber,K. and Osborn,M. (1991) A 210 kDa nuclear matrix protein is a functional part of the mitotic spindle; a microinjection study using SPN monoclonal antibodies. *EMBO J.*, **10**, 3351–3362.

Kallajoki,M., Weber,K. and Osborn,M. (1992) Ability to organize microtubules in taxol-treated mitotic PtK2 cells goes with the SPN antigen and not with the centrosome. *J. Cell Sci.*, **102**, 91–102.

Kallajoki,M., Harborth,J., Weber,K. and Osborn,M. (1993) Microinjection of a monoclonal antibody against SPN antigen, now identified by peptide sequences as the NuMA protein, induces micronuclei in PtK2 cells. *J. Cell Sci.*, **104**, 139–150.

Kroll,D.J., Abdel,M.A.H.H., Marcell,T., Simpson,S., Chen,C.Y., Gutierrez,H.A., Lustbader,J.W. and Hoeffler,J.P. (1993) A multifunctional prokaryotic protein expression system: overproduction, affinity purification, and selective detection. *DNA Cell Biol.*, **12**, 441–53.

Lydersen,B.K. and Pettijohn,D.E. (1980) Human-specific nuclear protein that associates with the polar region of the mitotic apparatus: distribution in a human/hamster hybrid cell. *Cell*, **22**, 489–499.

Maekawa,T. and Kuriyama,R. (1993) Primary structure and microtubule-interacting domain of the SP-H antigen: a mitotic MAP located at the spindle pole and characterized as a homologous protein to NuMA. *J. Cell Sci.*, **105**, 589–600.

Maekawa,T., Leslie,R. and Kuriyama,R. (1991) Identification of a minus end-specific microtubule-associated protein located at the mitotic poles in cultured mammalian cells. *Eur. J. Cell Biol.*, **54**, 255–267.

McIntosh,R.J. and Koonce,M.P. (1989) Mitosis. *Science*, **246**, 622–628.

Mizuno,T., Chou,M.Y. and Inouye,M. (1983) A comparative study on the genes for three porins of the *Escherichia coli* outer membrane: DNA sequence of the osmoregulated ompC gene. *J. Biol. Chem.*, **258**, 6932–6940.

Parry,D.A.D. (1994) NuMA/centrophilin: sequence analysis of the coiled-coil rod domain. *Biophys. J.*, **67**, 1203–1206.

Potschka,M., Nave,R., Weber,K. and Geisler,N. (1990) The two coiled coils in the isolated rod domain of the intermediate filament protein desmin are staggered; a hydrodynamic analysis of tetramers and dimers. *Eur. J. Biochem.*, **190**, 503–508.

Price,C.M. and Pettijohn,D.E. (1986) Redistribution of the nuclear mitotic apparatus protein (NuMA) during mitosis and nuclear assembly. *Exp. Cell Res.*, **166**, 295–311.

Sanger,F., Nicklen,S. and Coulson,A.R. (1977) DNA-sequencing with chain-terminating inhibitors. *Proc. Natl Acad. Sci. USA*, **74**, 5463–5467.

Schägger,H. and von Jagow,G. (1987) Tricine–sodium dodecyl sulfate–polyacrylamide gel electrophoresis for the separation of proteins in the range from 1 to 100 kDa. *Anal. Biochem.*, **166**, 368–379.

Stewart,M. and Edwards,P. (1984) Length of myosin rod and its proteolytic fragments determined by electron microscopy. *FEBS Lett.*, **168**, 75–78.

Stick,R. (1988) cDNA cloning of the developmentally regulated lamin LIII of *Xenopus laevis*. *EMBO J.*, **7**, 3189–3197.

Tang,T.K., Tang,C.C., Chen,Y.-L. and Wu,C.-W. (1993) Nuclear proteins of the bovine esophageal epithelium. II. The NuMA gene gives rise to multiple mRNAs and gene products reactive with monoclonal antibody W1. *J. Cell Sci.*, **104**, 249–260.

Tousson,A., Zeng,C., Brinkley,B.R. and Valdivia,M.M. (1991) Centrophilin: a novel mitotic spindle protein involved in microtubule nucleation. *J. Cell Biol.*, **112**, 427–440.

Yang,C.H. and Snyder,M. (1992) The nuclear-mitotic apparatus protein is important in the establishment and maintenance of the bipolar mitotic spindle apparatus. *Mol. Biol. Cell*, **3**, 1259–1267.

Yang,C.H., Lambie,E.J. and Snyder,M. (1992) NuMA: an unusually long coiled-coil related protein in the mammalian nucleus. *J. Cell Biol.*, **116**, 1303–1317.

Zeng,C., He,D. and Brinkley,B.R. (1994) Localization of NuMA protein isoforms in the nuclear matrix of mammalian cells. *Cell Motility Cytoskeleton*, **29**, 167–176.

*Received on January 31, 1995*